

# Nonlinear Multiple Models Adaptive Secondary Voltage Control of Microgrids

AQ1 Zixiao Ma<sup>1</sup>, Graduate Student Member, IEEE, Zhaoyu Wang<sup>1</sup>, Member, IEEE, Yifei Guo, Member, IEEE,  
 AQ2 Yuxuan Yuan<sup>1</sup>, Member, IEEE, and Hao Chen, Member, IEEE

1 **Abstract**—This article proposes a model-free secondary voltage  
 2 control (SVC) for microgrids (MG) using nonlinear multiple mod-  
 3 els adaptive control. Firstly, a linear robust adaptive controller  
 4 is designed to guarantee the voltage stability in the bounded-  
 5 input-bounded-output (BIBO) manner so as to meet the operation  
 6 requirements of MGs. Secondly, a nonlinear adaptive controller is  
 7 developed to improve the voltage tracking performance with the  
 8 help of artificial neural networks (ANNs). A switching mechanism  
 9 for coordinating such two controllers is designed to guaran-  
 10 tee the closed-loop stability while achieving accurate voltage  
 11 tracking. By an online identification based on the input and out-  
 12 put data of MGs, the proposed method does not resort to any  
 13 *a priori* information of system model and primary control, thus  
 14 exhibiting good robustness, ease of deployment and disturbance  
 15 rejection.

16 **Index Terms**—Artificial neural network (ANN), microgrid  
 17 (MG), multiple models, adaptive control, secondary voltage  
 18 control (SVC).

## NOMENCLATURE

### Abbreviations

21	ANN	Artificial neural network
22	BIBO	Bounded-input bounded-output
23	DER	Distributed energy resource
24	LAC	Linear adaptive controller
25	ARMAX	Auto-regressive moving average with exogenous input model
26	MG	Microgrid
27	MGCC	Microgrid central controller
28	NAC	Nonlinear adaptive controller
29	PI	Proportion-Integral
30	PV	Photovoltaic
31	SVC	Secondary voltage control
32	SNR	Signal-to-noise ratio.

### Variables

34	$J$	Objective function	34
35	$E^*$	Vector of voltage reference from SVC	35
36	$e_L, e_N$	Error vectors of linear and nonlinear models	36
37	$\bar{e}$	Voltage tracking error vector	37
38	$h$	Linear-transformed unmodeled dynamics	38
39	$\delta h, \hat{\delta h}$	Residual between real voltage and estimated voltage and its estimation using ANN	39
40	$k$	Time step index	40
41	$v_o^{\text{ref}}$	Predefined voltage reference	41
42	$v_o$	Vector of voltage magnitude	42
43	$v_{oi}$	Terminal voltage magnitude of the $i$ th DER	43
44	$v_{odi}, v_{oqi}$	$dq$ components of $v_{oi}$	44
45	$\hat{W}$	Estimation of the ideal weight matrix	45
46	$\Psi, \bar{\Psi}$	Vector of output and input voltage and its rearrangement	46
47	$y$	Linear transformed output voltage vector	47
48	$\hat{y}_L, \hat{y}_N$	Estimated transformed output voltage vectors using linear and nonlinear model identifier	48
49	$\Delta$	Positive constant	49
50	$\epsilon$	Small positive constant	50
51	$\mu$	Non-negative constant	51
52	$\Phi$	Unmodeled dynamics	52
53	$x$	Compact state variable vector of a MG	53
54	$\psi_i$	State vector of the $i$ th DER	54
55	$\xi$	Performance index of switching mechanism.	55

### Parameters

60	$A(\cdot)$	Matrix polynomial of $n$ th-order backward shift operator	60
61	$B(\cdot)$	Matrix polynomial of $(n - 1)$ th-order backward shift operator	61
62	$d$	Relative degree	62
63	$F(\cdot)$	Diagonal and stable weight matrix polynomial	63
64	$K(\cdot), L(\cdot)$	Matrix polynomials of $(n - 1)$ th-order	64
65	$m$	Number of DERs	65
66	$n$	MG system order	66
67	$R$	Diagonal real matrix	67
68	$\rho$	Bound of magnitude of unmodeled dynamics	68
69	$\theta$	Input-output parameter matrix	69
70	$\hat{\theta}_L, \hat{\theta}_N$	Estimated parameter matrices using linear and nonlinear models	70
71	$\Delta T$	Sampling time of secondary control.	71

AQ3 Manuscript received December 26, 2019; revised April 6, 2020 and  
 July 16, 2020; accepted September 7, 2020. This work was supported by  
 the U.S. Department of Energy Wind Energy Technologies Office under  
 Grant DE-EE0008956. Paper no. TSG-01929-2019. (Corresponding author:  
 Zhaoyu Wang.)

Zixiao Ma, Zhaoyu Wang, Yifei Guo, and Yuxuan Yuan are with the  
 Department of Electrical and Computer Engineering, Iowa State University,  
 Ames, IA 50011 USA (e-mail: zma@iastate.edu; wzy@iastate.edu;  
 yifeig@iastate.edu; yuanyx@iastate.edu).

AQ4 Hao Chen is with Tesla, Palo Alto, CA 94304 USA (e-mail:  
 haochengt16@gmail.com).

Color versions of one or more of the figures in this article are available  
 online at <http://ieeexplore.ieee.org>.

Digital Object Identifier 10.1109/TSG.2020.3023307

76 *Sets*

77  $\Omega$  Set of linear parameter matrix polynomials

78  $\mathbb{R}$  Set of real numbers.

## 79 I. INTRODUCTION

80 **M**ICROGRIDS (MGs) are localized small-scale power  
81 systems consisting of interconnected loads and dis-  
82 tributed energy resources (DERs), which can operate in both  
83 grid-connected and islanded modes. Compared with traditional  
84 fossil-fuel-based power grids, they have the advantages of fast  
85 demand response, low-carbon consumption, flexible utilization  
86 of DERs and high self-healing capability, etc [1], [2].

87 Despite of many benefits, MGs also bring some new control  
88 challenges. One of the key issues is the voltage tracking in the  
89 islanded mode. As known, *hierarchical control* is a popular  
90 choice for MGs, in which the *primary voltage control* with fast  
91 response maintains the stability while the *secondary voltage*  
92 *control (SVC)* corrects the voltage deviations [1], [2].

93 As per the control architecture and communication require-  
94 ments, MG control methods can be classified into three  
95 main categories: centralized, decentralized and distributed [3].  
96 Centralized approaches are usually implemented with a  
97 microgrid central controller (MGCC) and point-to-point com-  
98 munication network. It has well served the industry for decades  
99 and performs many practical merits. For instance, they are  
100 easy to implement and house and often less costly for small-  
101 scale systems [4]. Moreover, centralized architecture provides  
102 the best foundation for advanced control applications since  
103 all relevant data can be collected and processed in a single  
104 controller. However, it may suffer from single point of fail-  
105 ure [5]. Redundant communication systems can be installed to  
106 enhance the reliability; nonetheless, it will lead to additional  
107 cost [6]. Another solution is using decentralized or distributed  
108 control approaches. Decentralized control is implemented with  
109 local SVC controllers without communication network, assum-  
110 ing that the interactions between subsystems are negligible.  
111 However, this assumption does not always hold and might  
112 result in poor system-wide performance. Distributed control  
113 consists of local controllers and a sparse communication  
114 network. Averaging-based and consensus-based distributed  
115 SVC have been well investigated [7]. In the averaging-based  
116 SVC, each DER measures its required data and transmits them  
117 to all the other units [8]. The SVC signal is then calcu-  
118 lated by averaging the received data from other DERs [9].  
119 By employing the broadcast gossip algorithm, the required  
120 communication links can be reduced and the algorithm can  
121 converge to an equilibrium [10]. In the consensus-based SVC,  
122 the communication network is reduced more by transferring  
123 the required data just among the neighbor DERs [11]–[13].

124 Conventional SVC methods are based on *apriori* accurate  
125 models [14]. The input-output feedback linearization con-  
126 trol [15] that builds on the full knowledge of MG models  
127 and primary control might contradict the concept of hierar-  
128 chical control. Any changes of system structure or parameters  
129 could affect the control performance and could even result  
130 in instability. Some nonlinear control methods, e.g., model

predictive control [16], sliding mode control [17], internal  
model control [18], also have similar drawbacks. Several SVC  
strategies are designed based on specified models of primary  
controllers and inner controllers [3], [19]–[21], which restricts  
their generalization. A finite-time control-based method [22]  
was proposed to overcome such drawback. To alleviate the  
dependence on accurate models, robust control [23], predictive  
control [24], and variable-structure control [25] methods have  
been investigated. To overcome time-varying communication  
delays and communication noise disturbances, robust sec-  
ondary control approaches have been studied in [26], [27].  
However, partial model and uncertainty dynamics are still  
required for robust control and variable-structure control,  
though they do improve robustness.

145 Recently, *model-free* control has attracted a lot of atten-  
146 tion due to its advantages of robustness and flexibility [28].  
147 Reference [29] proposed a data-driven adaptive voltage control  
148 scheme for interlinking converters in interlinked hybrid ac/dc  
149 MGs, where the inner loop adopts a data-driven adaptive volt-  
150 age control and the SVC is essentially a Proportion-Integral  
151 (PI) controller. In [30], a bi-level distributed voltage con-  
152 trol scheme was proposed, where the high-level controller  
153 is designed for loss minimization; the low-level controller  
154 regulates the power output and terminal voltage. In [31],  
155 a model-free sliding mode control was adopted where the  
156 parameters are tuned with heuristic techniques, nevertheless,  
157 it suffers from chattering problem due the nature of sliding  
158 mode control [32]. Distributed averaging-based PI controllers  
159 for secondary frequency and voltage control were developed  
160 in [8], [9], [33]; however, they still require MG network  
161 information for controller parameter design.

162 Though most of SVC methods establish on linearized [5],  
163 [7], [11], [19] or nonlinear system models [3], [12], [20], [21],  
164 unfortunately, the detailed MG information including network  
165 topology, line impedances and loads, may be fully or par-  
166 tially unavailable to establish accurate models in some cases.  
167 Moreover, since there are uncertainty dynamics and distur-  
168 bances in DER-rich MGs, it is very hard to precisely capture  
169 such dynamics [34], [35]. Clearly, models with poor accu-  
170 racy can significantly deteriorate the control performance. For  
171 the existing model-free control methods, they mostly resort to  
172 PI control, which often suffers from high starting overshoot,  
173 high sensitivity to controller gains and sluggish response to  
174 disturbances [36].

175 *Our Contribution:* To address these challenges, we propose  
176 a multi-variable robust adaptive SVC method for MGs, which  
177 builds on the *multiple models* and *artificial neural networks*  
178 (*ANNs*) that are exploited to estimate the unmodeled dynam-  
179 ics of MGs. The controller consists of two separate linear and  
180 nonlinear modes that are coordinated by a tailored switch-  
181 ing strategy. In normal operation, the SVC operates under  
182 the nonlinear control mode which achieves the accurate volt-  
183 age tracking. It will switch to the linear control mode so as  
184 to guarantee the stability once there are large disturbances.  
185 The proposed method is inherently model-free, in the sense  
186 that it does not rely on *apriori* knowledge of MG topology,  
187 line impedances and load demands, which enables independ-  
188 ent designs between different control layers while enhancing

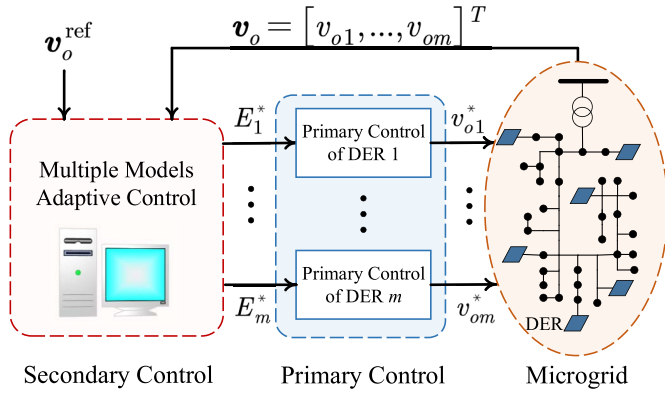


Fig. 1. Diagram of secondary and primary control structure of MG.

189 the robustness against uncertainties. We rigorously prove the  
 190 global *bounded-input-bounded-output (BIBO)* stability of the  
 191 controller and the equivalence between the tracking error and  
 192 identification error of unmodeled dynamics. This implies that  
 193 the accurate tracking can be achieved by properly designing  
 194 the hyper-parameters of ANNs. Besides, we also analyze and  
 195 test the robustness of the controller against time delays and  
 196 communication noise disturbances.

197 The remainder of this article is organized as follows.  
 198 Section II briefly introduces MGs with a hierarchical control  
 199 structure. Section III presents the model-free SVC along  
 200 with the closed-loop stability analysis. Simulation results are  
 201 presented in Section IV. Section V offers conclusions and  
 202 future directions. All of the technical proofs are collected in  
 203 the Appendix.

## 204 II. PROBLEM STATEMENT

### 205 A. Hierarchical Control of MGs

206 The hierarchical control structure is illustrated in Fig. 1.  
 207 Primary control generally results in voltage deviations since  
 208 it follows the droop control law. SVC is therefore used to  
 209 compensate the deviations of voltage. In the islanded mode,  
 210 the reference voltages, compactly denoted by  $\mathbf{V}_o^{\text{ref}}$ , are gen-  
 211 erally set as the nominal voltage of the MG, while in the  
 212 grid-tied mode, they are determined by the tertiary control [3].  
 213 SVC generates control inputs  $E_i^*$ ,  $i = 1, \dots, m$ , according to  
 214 the references and they are dispatched to each local primary  
 215 controller of DERs. Then, the primary control calculates the  
 216 voltage reference  $v_{oi}^*$  for the local inner control loops. Finally,  
 217 the measured output voltages of DERs  $v_{oi}$  are measured and  
 218 fed back to the SVC.

219 The secondary control has much slower dynamic response  
 220 compared to primary control, which decouples the primary  
 221 and secondary control [2]. This enables independent controller  
 222 design at different layers. However, the flexibility of primary  
 223 control is always limited to guarantee control performance  
 224 when model-based control algorithms (e.g., feedback lineariza-  
 225 tion and sliding mode control) are applied in the secondary  
 226 layer. The a priori structures and parameters of primary control  
 227 should be considered in SVC design and uncertainties  
 228 and disturbances of primary layer could lead to instability and  
 229 large tracking errors of MGs. This motivates us to develop a

230 robust model-free SVC without knowing any specifications of  
 231 primary layer.

### 232 B. Islanded MG System Description

233 In an islanded MG, the primary and inner control structures  
 234 of inverter-based DERs are shown in Fig. 2. In the islanded  
 235 mode, the control input of primary droop voltage controller is  
 236  $E_i^*$ ,  $\forall i$ , which is obtained from SVC and the system output is  
 237 the terminal voltage  $v_{oi}$ . Such MG system can be compactly  
 238 expressed by a nonlinear state-space model as,

$$239 \quad \dot{\mathbf{x}}(t) = f(\mathbf{x}(t), \mathbf{E}^*(t)) \quad (1a)$$

$$240 \quad \mathbf{v}_o(t) = g(\mathbf{x}(t)) \quad (1b)$$

241 where  $\mathbf{v}_o := [v_{o1}, \dots, v_{om}]^T$ ;  $\mathbf{x} := [x_1^T, \dots, x_m^T]^T$ ;  
 242  $\mathbf{E}^* := [E_1^*, \dots, E_m^*]^T$ ;  $\mathbf{x}_i$  denotes the internal state variables of  
 243  $i$ th DER;  $f$  and  $g$  are the functions representing the nonlinear  
 244 dynamic system.

245 *Remark 1:* Note that, Fig. 2 is only used to illustrate how  
 246 the control signal  $E_i^*$  acts on the primary control layer, which  
 247 is actually not needed for our SVC design benefiting from the  
 248 model-free nature. In addition, this article focuses on SVC, so  
 249 the design of frequency control is not limited, which also gives  
 250 freedom to primary control, e.g., the PLL may not be needed  
 251 when droop characteristics control the frequency [37]. Besides,  
 252 functions  $f$  and  $g$  and state variables  $\mathbf{x}$  are not necessarily  
 253 required.

## 254 III. MODEL-FREE SVC BASED ON NONLINEAR MULTIPLE 255 MODELS ADAPTIVE CONTROL

256 In this section, a novel SVC method based on nonlinear  
 257 multiple models adaptive control with unmodeled dynamics is  
 258 proposed. We first present the design of linear and nonlinear  
 259 controllers, respectively. Then, the controller parameter iden-  
 260 tification method is given. Finally, a switching mechanism is  
 261 designed to coordinate the linear and nonlinear parts.

### 262 A. Optimal Controller Design for Voltage Regulation

263 Given that the measurements are sampled, system (1) are  
 264 discretized as,

$$265 \quad \mathbf{x}(k+1) = f(\mathbf{x}(k), \mathbf{E}^*(k)), \quad (2a)$$

$$266 \quad \mathbf{v}_o(k) = g(\mathbf{x}(k)), \quad (2b)$$

267 where  $\mathbf{E}^* \in \mathbb{R}^m$ ,  $\mathbf{v}_o \in \mathbb{R}^m$ ,  $\mathbf{x} \in \mathbb{R}^n$ . The origin is an equilibrium  
 268 of function  $f$  and  $g$ .

269 If system (2) is observable for  $n$ th order, the state variables  
 270 of MGs  $\mathbf{x}(k)$  can be expressed as a function of input and output  
 271 variables,  $\mathbf{v}_o(k), \dots, \mathbf{v}_o(k-n+1), \mathbf{E}^*(k), \dots, \mathbf{E}^*(k-n+1)$ .  
 272 Thus, (2) can be represented with only voltage control inputs  
 273 and voltage outputs by the auto-regressive moving-average  
 274 with exogenous input (ARMAX) model as,

$$275 \quad \mathbf{A}(z^{-1})\mathbf{v}_o(k+d) = \mathbf{B}(z^{-1})\mathbf{E}^*(k) \\ 276 \quad + \boldsymbol{\varphi}[\mathbf{v}_o(k+d-1), \dots, \mathbf{v}_o(k+d-n), \\ 277 \quad \mathbf{E}^*(k), \dots, \mathbf{E}^*(k-n+1)]], \quad (3)$$

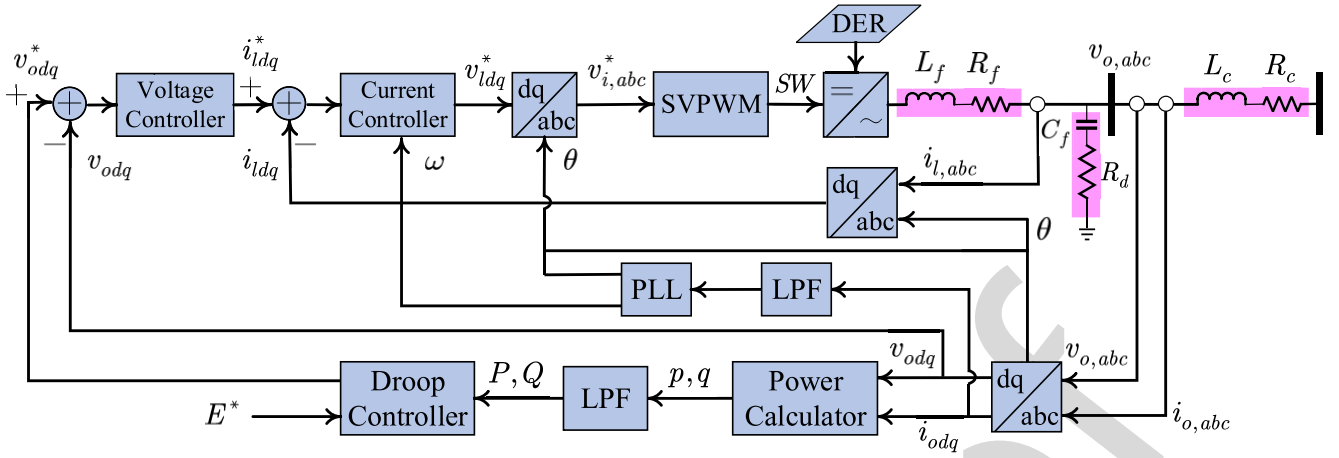


Fig. 2. The diagram of control structure of the VSC-based DER. PLL denotes the phase-locked loop; LPF denotes the low-pass filter; SVPWM denotes the space vector pulse width modulation.

where  $\mathbf{A}(z^{-1})$  is a  $m \times m$  matrix polynomial of  $n$ th-order backward shift operator;  $\mathbf{B}(z^{-1})$  is a  $m \times m$  matrix polynomial of  $(n-1)$ th-order backward shift operator;  $d$  ( $1 \leq d \leq n$ ) is the relative degree;  $\boldsymbol{\varphi}[\cdot] \in \mathbb{R}^n$  is the unmodeled dynamics, which is a higher-order nonlinear function of  $\mathbf{v}_o(k), \dots, \mathbf{v}_o(k-n+1), \mathbf{E}^*(k), \dots, \mathbf{E}^*(k-n+1)$  [38].  $n$  and  $d$  are unknown if the detailed model of primary controllers and MGs are not available. However, they can be determined by the method in [39]. Moreover, the following assumptions are widely believed to hold for MGs in practice.

*Assumption 1:* (i) The internal dynamics of MGs are globally uniformly asymptotically stable; (ii) matrix polynomials  $\mathbf{A}(z^{-1})$  and  $\mathbf{B}(z^{-1})$  lie in a closed and bounded set  $\Omega$ .

Assumption 1(i) ensures that the voltage control input  $\mathbf{E}^*$  will not grow faster than the output voltage  $\mathbf{v}_o$ , indicating the MG is a minimum-phase system. Note that, this assumption is not necessary if the linear part of system (2) is asymptotically stable and thus, the proposed method can be applied to this kind of non-minimum-phase nonlinear system [40].

To ensure the stability while improving the voltage tracking performance, two separate optimal controllers are designed. We first define a cost function on voltage tracking errors,

$$J := \left\| \mathbf{F}(z^{-1})\mathbf{v}_o(k+d) - \mathbf{R}\mathbf{v}_o^{\text{ref}}(k) \right\|^2, \quad (4)$$

where  $\mathbf{v}_o^{\text{ref}} \in \mathbb{R}^m$  is voltage reference vector;  $\mathbf{F}(\cdot)$  denotes a  $m \times m$  weight matrix polynomial, which is stable and diagonal;  $\mathbf{R}$  is a  $m \times m$  diagonal real matrix.

To minimize (4), an optimal control law is designed as,

$$\mathbf{L}(z^{-1})\mathbf{B}(z^{-1})\mathbf{E}^*(k) + \mathbf{K}(z^{-1})\mathbf{v}_o(k) + \mathbf{h}[\cdot] = \mathbf{R}\mathbf{v}_o^{\text{ref}}(k) \quad (5)$$

where  $\mathbf{L}(z^{-1})$  denotes a  $m \times m$   $(n-1)$ th order polynomial,  $\mathbf{K}(z^{-1}) := \mathbf{K}_0 + \mathbf{K}_1z^{-1} + \dots + \mathbf{K}_{n-1}z^{-n+1}$  is a  $m \times m$  matrix polynomial and  $\mathbf{h}[\cdot] := \mathbf{L}(z^{-1})\boldsymbol{\varphi}[\cdot]$ .  $\mathbf{L}(z^{-1})$  and  $\mathbf{K}(z^{-1})$  can be calculated by,

$$\mathbf{F}(z^{-1}) = \mathbf{L}(z^{-1})\mathbf{A}(z^{-1}) + z^{-d}\mathbf{K}(z^{-1}). \quad (6)$$

$\mathbf{h}[\cdot]$  in (5) is a linear transformation of unmodeled dynamics  $\boldsymbol{\varphi}[\cdot]$ , which can be estimated using ANNs. Let  $\hat{\mathbf{h}}[\cdot]$  be its

estimation, and then substitute (5) into (3), one can obtain, 313

$$\mathbf{F}(z^{-1})\mathbf{v}_o(k+d) = \mathbf{R}\mathbf{v}_o^{\text{ref}}(k) + \mathbf{h}[\cdot] - \hat{\mathbf{h}}[\cdot] \quad (7) \quad 314$$

where  $\mathbf{F}(z^{-1})$  can be selected as a diagonal matrix such that its characteristic polynomial describes the poles of (7) and  $\mathbf{R}$  can be chosen as  $\mathbf{F}(1)$ . If we obtain the linear parts of the system, the tracking error  $\bar{\mathbf{e}} = \mathbf{F}(z^{-1})\mathbf{v}_o(k+d) - \mathbf{R}\mathbf{v}_o^{\text{ref}}(k)$  of the closed-loop system equals  $\mathbf{h}[\cdot] - \hat{\mathbf{h}}[\cdot]$ . With proper configuration of the ANNs,  $\bar{\mathbf{e}}$  can be controlled to be arbitrarily small [38]. 315 316 317 318 319 320

If the high-order nonlinear term  $\mathbf{h}[\cdot]$  is small enough, (5) can be simplified as a linear control law as, 321 322

$$\mathbf{L}(z^{-1})\mathbf{B}(z^{-1})\mathbf{E}^*(k) + \mathbf{K}(z^{-1})\mathbf{v}_o(k) = \mathbf{R}\mathbf{v}_o^{\text{ref}}(k). \quad (8) \quad 323$$

## B. Multiple Models Adaptive Control Based on ANNs 324

1) *Identification of Controller Parameters:* To achieve model-free control with *unknown* MG parameters, we propose to exploit the adaptive control method. From (3) and (6), we can obtain 325 326 327 328

$$\mathbf{y}(k+d) = \boldsymbol{\theta}^T \boldsymbol{\Psi}(k) + \mathbf{h}[\bar{\boldsymbol{\Psi}}(k)], \quad (9) \quad 329$$

where  $\mathbf{y}(k+d) := \mathbf{F}(z^{-1})\mathbf{v}_o(k+d)$  denotes the transformed output voltage;  $\boldsymbol{\theta} := [\mathbf{K}_0, \dots, \mathbf{K}_{n-1}, \mathbf{L}\mathbf{B}_0, \dots, \mathbf{L}\mathbf{B}_{n+d-2}]^T$  denotes the input-output parameter matrix;  $\boldsymbol{\Psi}(k) := [\mathbf{v}_o(k)^T, \dots, \mathbf{v}_o(k-n+1)^T, \mathbf{E}^*(k)^T, \dots, \mathbf{E}^*(k-n-d+2)^T]^T$  is the vector collecting all the output and input voltages, and  $\bar{\boldsymbol{\Psi}}(k) = [\mathbf{v}_o(k), \dots, \mathbf{v}_o(k-n+1), \mathbf{E}^*(k), \dots, \mathbf{E}^*(k-n-d+2)]$ . From Assumptions 1(ii), one can know that the parameter matrix  $\boldsymbol{\theta}$  lies in a certain closed and bounded set. Assuming the unmodeled dynamics  $\mathbf{h}[\cdot]$  are globally bounded by a known positive constant  $\rho$ , i.e.,  $\|\mathbf{h}[\cdot]\| \leq \rho$ , we propose the linear and nonlinear model estimators for parameter identification. The linear estimator is designed as, 330 331 332 333 334 335 336 337 338 339 340 341

$$\hat{\mathbf{y}}_L(k+d) = \hat{\boldsymbol{\theta}}_L(k)^T \boldsymbol{\Psi}(k) \quad (10) \quad 342$$

where  $\hat{\mathbf{y}}_L$  and  $\hat{\boldsymbol{\theta}}_L(k)$  are linear estimated transformed output voltage and linear estimated parameter vectors, respectively. 343 344

345 The update law is designed as,

$$346 \quad \hat{\theta}_L(k) = \text{proj}\{\hat{\theta}'_L(k)\}, \quad (11)$$

$$347 \quad \hat{\theta}'_L(k) = \hat{\theta}_L(k-d) + \frac{\eta_L(k)\Psi(k-d)e_L(k)^T}{1 + \|\Psi(k-d)\|^2}, \quad (12)$$

$$348 \quad \eta_L(k) = \begin{cases} 1 & \text{if } \|e_L(k)\| > 2\rho, \\ 0 & \text{otherwise,} \end{cases} \quad (13)$$

349 where  $e_L(k)$  is the identification error of linear model, i.e.,

$$350 \quad e_L(k) = \mathbf{y}(k) - \hat{\theta}_L(k-d)^T \Psi(k-d), \quad (14)$$

$$351 \quad \hat{\theta}'_L(k) = [\hat{\mathbf{K}}_{1,0}(k), \dots, \hat{\mathbf{K}}_{1,n-1}(k), \hat{\mathbf{L}}'_{1,0}(k) \hat{\mathbf{B}}'_{1,0}(k), \dots, \\ 352 \quad \hat{\mathbf{L}}'_{1,n+d-2}(k) \hat{\mathbf{B}}'_{1,n+d-2}(k)]^T; \text{proj}\{\cdot\} \text{ is a projection operator as}$$

$$353 \quad \text{proj}\{\hat{\theta}'_L(k)\} = \begin{cases} \hat{\theta}'_L(k) & \text{if } |\hat{\mathbf{L}}'_{1,0}(k) \hat{\mathbf{B}}'_{1,0}(k)| \geq h_{\min}, \\ [\dots, h_{\min}, \dots]^T & \text{otherwise,} \end{cases} \quad (15)$$

355 where  $h_{\min} > 0$  is defined based on prior knowledge. This  
356 aims to prevent the control signal from being too big due to  
357 the too small identification parameter  $\hat{\mathbf{L}}'_{1,0}(k) \hat{\mathbf{B}}'_{1,0}(k)$ .

358 The nonlinear estimator is designed as,

$$359 \quad \hat{\mathbf{y}}_N(k+d) = \hat{\theta}_N(k)^T \Psi(k) + \delta \hat{\mathbf{h}}[\bar{\Psi}(k)], \quad (16)$$

360 where  $\hat{\mathbf{y}}_N$  and  $\hat{\theta}_N$  are nonlinear estimated transformed output  
361 voltage and nonlinear estimated parameter vectors, respec-  
362 tively.  $\delta \hat{\mathbf{h}}[\bar{\Psi}(k)]$  is the estimation of  $\delta \mathbf{h}[\bar{\Psi}(k)]$  by ANNs at time  
363 instant  $k$  with  $\delta \mathbf{h}[\bar{\Psi}(k)] = \mathbf{y}(k+d) - \hat{\theta}_N(k)^T \Psi(k)$ . According  
364 to [41], the only requirement on the update laws of  $\hat{\theta}_N(k)$  and  
365  $\hat{\mathbf{W}}(k)$  is that they always lie in certain compact set. Hence, the  
366 update law of  $\hat{\theta}_N(k)$  is designed similar to that of  $\hat{\theta}_L(k)$  where  
367 the difference is the definition of identification error, i.e.,

$$368 \quad e_N(k) = \mathbf{y}(k) - \hat{\theta}_N(k-d)^T \Psi(k-d) - \delta \hat{\mathbf{h}}[\bar{\Psi}(k-d)]. \quad (17)$$

369 2) *Nonlinear Identifier and Controller Based on ANNs:*

370 The voltage tracking performance of MGs heavily depends on  
371 the accuracy of estimation of the unmodeled dynamics, i.e.,  
372  $\delta \mathbf{h}[\bar{\Psi}(k)]$ . As reported in [41], [42], ANNs are the universal  
373 approximators. Hence, by a proper choice of the structure and  
374 parameters of ANNs, the identification error of unmodeled  
375 dynamics  $\|\delta \hat{\mathbf{h}} - \delta \mathbf{h}[\bar{\Psi}(k)]\|$  can be made arbitrarily small over  
376 a compact set. We choose the back propagation (BP) ANN to  
377 estimate the unmodeled dynamics  $\delta \mathbf{h}[\bar{\Psi}(k)]$ .

378 To guarantee that the hyper-parameters are well-tuned, we  
379 use the random search algorithm in [43] to calibrate the  
380 hyper-parameters based on the performance on a validation  
381 set. According to [38], with well-tuned hyper-parameters and  
382 appropriate training algorithm, one can obtain the estimation of  
383 ideal parameter matrix,  $\hat{\mathbf{W}}(k)$  (containing weights and biases).  
384 Then, by taking  $\hat{\mathbf{W}}(k)$  and  $\Psi(k)$  as the input vectors of the  
385 ANN function, it can achieve accurate and fast estimation of  
386 unmodeled dynamics. From a system theoretical point of view,  
387 ANNs are convenient families of nonlinear mappings as,

$$388 \quad \delta \hat{\mathbf{h}}[\bar{\Psi}(k)] = \phi[\hat{\mathbf{W}}(k), \Psi(k)] \\ 389 \quad = \hat{\mathbf{W}}_3(k) \Gamma(\hat{\mathbf{W}}_2(k) \Gamma(\hat{\mathbf{W}}_1(k) \Psi(k) + \hat{\mathbf{b}}_1) + \hat{\mathbf{b}}_2) \\ 390 \quad + \hat{\mathbf{b}}_3 \quad (18)$$

391 where  $\phi[\cdot]$  represents the function of ANNs;  $\hat{\mathbf{W}}_i$  and  $\hat{\mathbf{b}}_i$  denote  
392 the ideal weight and bias vectors, respectively,  $i = 1, 2, 3$ ;  $\Gamma$   
393 represents a vector of activation functions.

394 3) *Linear Adaptive Controller and ANN-Based Nonlinear*  
395 *Adaptive Controller:* Finally, the linear adaptive controller  
396 (LAC) is designed as

$$397 \quad \hat{\theta}_L(k)^T \Psi(k) = \mathbf{R} \mathbf{v}_o^{\text{ref}}(k). \quad (19)$$

398 Moreover, the nonlinear adaptive controller (NAC) based on  
399 ANN is designed as

$$400 \quad \hat{\theta}_N(k)^T \Psi(k) + \delta \hat{\mathbf{h}}[\bar{\Psi}(k)] = \mathbf{R} \mathbf{v}_o^{\text{ref}}(k). \quad (20)$$

401 4) *Controller Design for Time Delays:* In hierarchical control,  
402 the sampling time of SVC is larger than the primary  
403 control. The communication delays between the two levels can  
404 affect the stability and tracking performance of MGs. So, we  
405 consider a discrete-time system whose sampling time is equal  
406 to that of voltage measurement. We round the time delays to  
407 an integer multiple of the sampling period.

408 When there is no communication delay, i.e.,  $d = 1$ , the  
409 predicted output  $\hat{\mathbf{v}}_o(k)$  is computed with  $\hat{\theta}(k-1)$ . However,  
410 when time delay exists, i.e.,  $d > 1$ , the measured output  
411 voltage  $\mathbf{v}_o(k)$  depends on the control input  $\mathbf{E}^*(k-d)$  which  
412 is calculated with estimated parameters  $\hat{\theta}(k-d)$  using the  
413 then available measurement. Therefore, the identification error  
414  $\mathbf{e}(k)$  using  $\hat{\theta}(k-1)$  is equal to the tracking error  $\bar{\mathbf{e}}(k)$  with  
415 delayed measurements. To solve this problem, the update law  
416 is designed in the form of (11)–(13). It can be elaborated that  
417 the sequence  $\hat{\theta}(k)$  are divided into  $d$  subsequences and each  
418 one updates itself when data is available. Note that,  $\hat{\mathbf{W}}$  in (18)  
419 also needs to be split into  $d$  sequences and the corresponding  
420 ANNs update their parameters in their own time-scale.

### 421 C. Switching Mechanism

422 LAC aims to guarantee the stability while NAC is designed  
423 to achieve accurate voltage tracking. As shown in Fig. 3, the  
424 error between the weighted output voltage  $\mathbf{F} \mathbf{v}_o$  of MGs and  
425 weighted desired voltage reference  $\mathbf{R} \mathbf{v}_o^{\text{ref}}$  are given to the lin-  
426 ear and nonlinear loops simultaneously at each time step  $k$ . In  
427 the nonlinear loop, NAC generates the voltage control signals  
428  $\mathbf{E}_{Ni}^*$  and transfers it to the nonlinear identified model based on  
429 ANNs. It is the same for the linear loop except that the con-  
430 troller and identifier are replaced by LAC and ARMAX model  
431 without ANN. Then, both linear and nonlinear identification  
432 errors,  $e_L$  and  $e_N$ , are sent to the switching logic block. This  
433 block decides which controller is selected in the current time  
434 step. Finally, the selected voltage control signal is adopted in  
435 the primary control of DERs.

436 The performance index of switching mechanism is proposed  
437 based on a similar logic in [41]:

$$438 \quad \xi_j(k) = \sum_{s=d}^k \frac{\eta_j(s) (\|e_j(s)\|^2 - 4\rho^2)}{2(1 + \|\Psi(s-d)\|^2)} \\ 439 \quad + \mu \sum_{s=k-M+1}^k (1 - \eta_j(s)) \|e_j(s)\|^2 \quad (21)$$

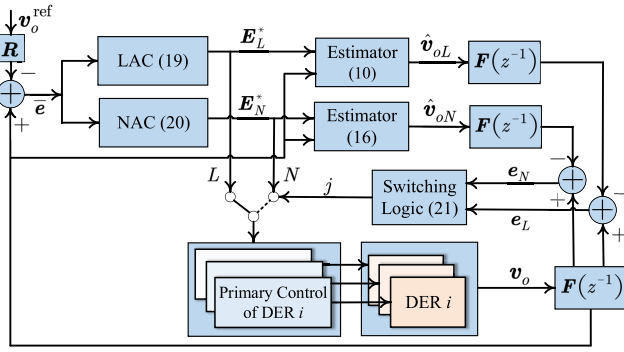


Fig. 3. The diagram of closed-loop MG system with proposed SVC using nonlinear multiple models adaptive control. When  $j$  switches to 'L', the linear estimator and controller are used; otherwise, the nonlinear ones are selected.

$$\eta_j(k) = \begin{cases} 1 & \text{if } \|e_j(s)\| > 2\rho, \\ 0 & \text{otherwise,} \end{cases} \quad (22)$$

where  $\mu \geq 0$  is a constant and  $M$  is a positive integer. We select the linear or nonlinear controller according to the smaller performance index:

$$\xi_* = \min[\xi_L, \xi_N]. \quad (23)$$

Note that, the performance index (21) is comprised of two terms. The first term is designed to differentiate signals with different rates to guarantee the boundedness of all signals, thus realizing stable switching. The second term is a measure of estimation errors over a period and is used to improve control performance [41]. When the linear or nonlinear identifier predicts the voltage with smaller errors, the second term decreases, thus the corresponding controller will be chosen. Properly selecting  $\mu$  and  $\rho$  can enhance the stability. An outstanding advantage of such switching mechanism is that the stability and tracking performance can be decoupled. This means the hyper-parameters and training method of ANNs do not affect the stability.

When the ANN is degraded or disturbed,  $e_N$  increases. Consequently,  $\xi_L < \xi_N$  and LAC is chosen. LAC keeps working to guarantee the stability until the ANN-based controller recovers. As  $e_N$  decreases,  $\xi_L$  is greater than  $\xi_N$  and the controller NAC is chosen to improve the performance. A proper selection of  $\mu$  and  $\rho$  can enhance the voltage tracking performance while guaranteeing closed-loop stability.

*Remark 3:* According to the switched systems theory [44], it is possible to guarantee the stability with better performance by frequently switching controllers for unstable subsystems. However, such frequent switching may deteriorate the control performance or even cause instability in subsystems. Therefore, designing an appropriate switching mechanism is essential [45]. Our switching mechanism considers both the stability and voltage tracking performance.

#### D. Analysis of Stability and Tracking Error Convergence

In this section, we analyze the stability and voltage tracking errors of the closed-loop MG system with the proposed SVC method, which are detailed by the following propositions.

*Proposition 1 (BIBO-Stability):* For the system (3) with the control algorithm (10)–(22), suppose Assumption 1 holds and

#### Algorithm 1 Model-Free SVC

- 1: Measure the MG output voltage  $v_o(k)$  and establish data vector  $\Psi(k-d)$  together with SVC input  $E^*(k)$  at current time step.
- 2: **procedure** CONTROLLER SELECTION
- 3: Calculate the identification errors  $e_L(k)$  and  $e_N(k)$  using (14) and (17), respectively.
- 4: Calculate  $\xi_L(k)$  and  $\xi_N(k)$  with (21) and (22).
- 5: **if**  $\xi_L(k) \leq \xi_N(k)$  **then**
- 6:  $j$  switches to position  $L$  and select linear controller
- 7: **else**
- 8: Let  $j = N$  and select nonlinear controller.
- 9: **end if**
- 10: **end procedure**
- 11: **procedure** CONTROLLER CALCULATION
- 12: **if**  $j = L$  **then**
- 13: Estimate LAC parameters  $\hat{\theta}_L(k)$  with (11)–(15), and calculate the SVC input  $E^*(k)$  using (19).
- 14: **else**
- 15: Estimate NAC parameters  $\hat{\theta}_N(k)$  with (17)–(18) and calculate  $E^*(k)$  using (20).
- 16: **end if**
- 17: **end procedure**
- 18: Let  $k = k + 1$ , and return to Step 1.

$\|h[\cdot]\| \leq \rho$ , the inputs  $E^*$  and output voltages  $v_o$  of MGs are uniformly bounded, i.e.,

$$\max_{0 \leq \tau \leq k} \{\|v_o(\tau)\|, \|E^*(\tau)\|\} \leq \Delta \quad (24)$$

which holds for some positive constant  $\Delta$ .

There are many kinds of stability definitions, such as Lyapunov stability, asymptotic stability, etc. For MG system which is nonlinear, these stability definitions only require the voltages converge to the stable operation point without boundedness. However, in practical operation, it is more important to ensure the voltage not to exceed the stability bound rather than to converge in infinite time. Therefore, in this article, we define the stability in a BIBO manner, which guarantees that all the output voltages of MGs are bounded. It is worth noting that our proposed control strategy naturally guarantees the inputs are bounded, which implies our method is much feasible in practice.

*Proposition 2 (Tracking Error Convergence):* With proper hyper-parameter calibration of ANNs and the proposed adaptive control method, the voltage tracking errors asymptotically converge to an arbitrarily small positive constant  $\epsilon$ , i.e.,

$$\lim_{k \rightarrow \infty} \|\bar{e}(k)\| = \lim_{k \rightarrow \infty} \|F(z^{-1})v_o(k) - Rv_o^{\text{ref}}(k-d)\| < \epsilon.$$

The proofs can be found in the Appendix.

#### E. Algorithm Implementation

The overall SVC algorithm design is presented in Algorithm 1. Firstly,  $v_o(k)$  is measured and sent to the SVC controller. The sampling rate of secondary control can be chosen from 100 Hz to 1 kHz [46]. Combining  $v_o(k)$  and  $E^*(k)$  with the historical data, we construct the data vector  $\Psi(k-d)$ . The number of historical data depends on the  $n$  and  $d$ , which can be identified using the method in [39]. Then, the linear and nonlinear identifiers and controllers are established in the control center. The parameters  $\rho$  and  $\mu$  in (21)–(23) can affect the

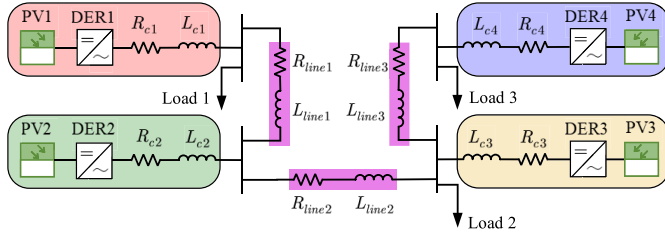


Fig. 4. MG test system.

 TABLE I  
 PI PARAMETERS OF DERs

Controller	Parameter	Value	Parameter	Value
Voltage Controller	$K_{PV1}$	0.5	$K_{IV1}$	52
	$K_{PV2}$	0.5	$K_{IV2}$	52
	$K_{PV3}$	0.25	$K_{IV3}$	34
	$K_{PV4}$	0.25	$K_{IV4}$	34
Current Controller	$K_{PC1}$	4.5	$K_{IC1}$	450
	$K_{PC2}$	4.5	$K_{IC2}$	450
	$K_{PC3}$	3.55	$K_{IC3}$	353
	$K_{PC4}$	3.55	$K_{IC4}$	353

 TABLE II  
 MG PARAMETERS

Parameter	Value	Parameter	Value
$L_{f1}, L_{f2}$	3.9 mH	$L_{f3}, L_{f4}$	3.9 mH
$R_{f1}, R_{f2}$	0.50 $\Omega$	$R_{f3}, R_{f4}$	0.50 $\Omega$
$L_{c1}, L_{c2}$	0.35 mH	$L_{c3}, L_{c4}$	0.45 mH
$R_{c1}, R_{c2}$	0.08 $\Omega$	$R_{c3}, R_{c4}$	0.09 $\Omega$
$C_{f1}, C_{f2}$	16 $\mu$ F	$C_{f3}, C_{f4}$	16 $\mu$ F
$R_{d1}, R_{d2}$	2.05 $\Omega$	$R_{d3}, R_{d4}$	2.05 $\Omega$
$D_{Q1}$	$1 \times 10^{-3}$ V/Var	$D_{Q2}$	$1 \times 10^{-3}$ V/Var
$D_{Q3}$	$1.5 \times 10^{-3}$ V/Var	$D_{Q4}$	$1.5 \times 10^{-3}$ V/Var
$R_{line1}$	0.15 $\Omega$	$L_{line1}$	0.42 mH
$R_{line2}$	0.35 $\Omega$	$L_{line2}$	0.33 mH
$R_{line3}$	0.23 $\Omega$	$L_{line3}$	0.55 mH
$P_{load1}$	20 kW	$Q_{load1}$	9 kVar
$P_{load2}$	16 kW	$Q_{load2}$	9 kVar
$P_{load3}$	12 kW	$Q_{load3}$	6 kVar

511 tracking performance. As  $\rho$  decreases, the accuracy of linear  
 512 parts increases. But if  $\rho$  is too small, the parameter updating  
 513 process converges slowly.  $\mu$  represents the weight of tracking  
 514 performance. To balance the stability and control performance,  
 515  $\mu$  is usually selected around 1.5 [38]. The widely-used two-  
 516 way communication network between MGCC and DERs is  
 517 required [47].

#### 518 IV. CASE STUDIES

##### 519 A. Simulation Setup

520 The proposed SVC is tested on a widely used MG system  
 521 (see Fig. 4), originally consisting of four inverter-based DERs  
 522 and two loads [48]. The control system of DERs has been  
 523 shown in Fig. 2. The MG parameters are given in Table II.  
 524 The sampling periods of primary and secondary control are  
 525 set as  $10^{-4}$  s and 0.01 s, respectively. The total simulation  
 526 time is 10 s. All the dynamic simulations are implemented in  
 527 MATLAB/Simulink environment.

528 We establish a feed-forward ANN consisting of two hidden  
 529 layers (50 and 8 nodes, respectively). To obtain the training  
 530 set, we first only adopt the LAC and make  $\mathbf{v}_o^{\text{ref}}$  time-varying  
 531 instead of a constant. When finishing this case, we select the

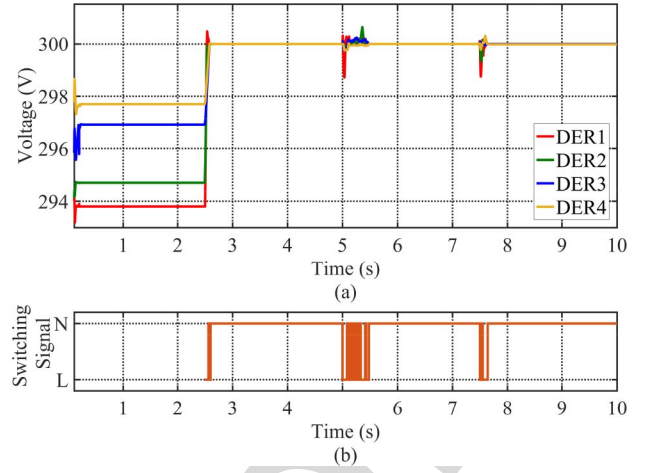


Fig. 5. Voltage tracking performance of the proposed controller.

532 current and historical control inputs  $\mathbf{E}^*(k), \dots, \mathbf{E}^*(k-n+1)$ ,  
 533  $k = 1, \dots, 1000$  and output voltages  $\mathbf{v}_o(k+d-1), \dots, \mathbf{v}_o(k+d-n)$   
 534 as the inputs of the training of ANN. While the errors between the output  
 535 voltage of the linear model with LAC and real voltages  $h(\tilde{\Psi}(k)) = \mathbf{v}_o(k+d) - \hat{\mathbf{v}}_o(k+d) =$   
 536  $\mathbf{y}(k) - \hat{\boldsymbol{\theta}}_L(k)^T \tilde{\Psi}(k)$  are used as the output of the training  
 537 set. The ANN is trained offline using back-propagation with  
 538 Levenberg-Marquardt algorithm [49]. The learning rate is set  
 539 as  $lr = 0.9$ , and the momentum factor is selected as  $mc = 0.8$ .  
 540 The activation function for the first and second hidden layers  
 541 are selected as “tansig” and “purelin”, respectively. The  
 542 offline training of ANN takes 29.36 s and 1675 iterations.  
 543 The mean squared error of training and test are  $9.94 \times 10^{-6}$   
 544 and  $3.85 \times 10^{-3}$ , respectively. The trained ANN is integrated  
 545 into the NAC as an identifier.  
 546

##### 547 B. Tracking Performance

548 The voltage tracking performance is shown in Fig. 5. The  
 549 reference voltages are set as 300 V. The SVC is not applied  
 550 until  $t = 2.5$  s. Before that though voltages are stable, steady  
 551 state errors still exist. Once SVC is implemented, the volt-  
 552 age magnitudes are restored to the reference values rapidly.  
 553 At  $t = 5$  s, a constant power load is attached to the system.  
 554 To show the robustness of the model-free method, a parame-  
 555 ter perturbation that  $L_{c1}$  is reduced by 25% is triggered since  
 556  $t = 7.5$  s. From Fig. 5(b), we notice that when large distur-  
 557 bances happen, the control mode oscillates between the  
 558 LAC and NAC due to the degradation of ANNs. The switch-  
 559 ing mechanism is trying to balance the tracking performance  
 560 and stability. Once ANN recovers, it switches back to NAC.  
 561 The results show that the proposed SVC exhibits good voltage  
 562 tracking performance and robustness to the uncertain pertur-  
 563 bations. Fig. 6 shows that the active power outputs of DERs  
 564 are allocated according to their rated power.

##### 565 C. Stability of LAC

566 One may doubt that what if the ANN is not well-trained or  
 567 its hyper-parameters are not well-tuned. To verify the stabi-  
 568 lization of the proposed controller, we only use the LAC by

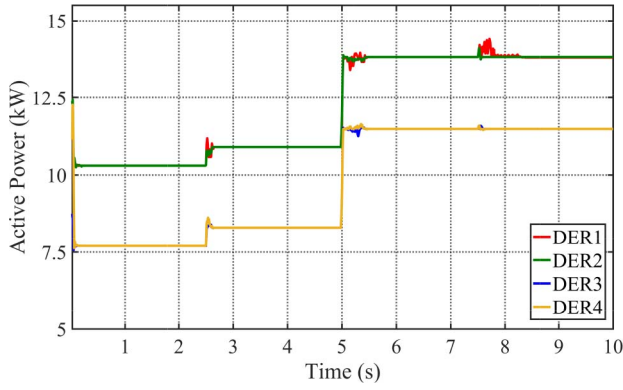


Fig. 6. Active power outputs using multiple models adaptive control.

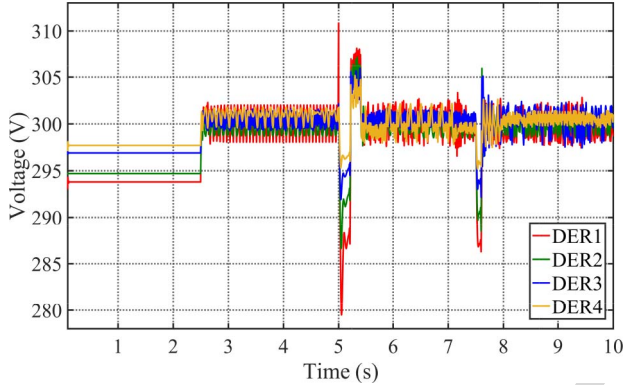


Fig. 7. Stability performance of voltage using LAC.

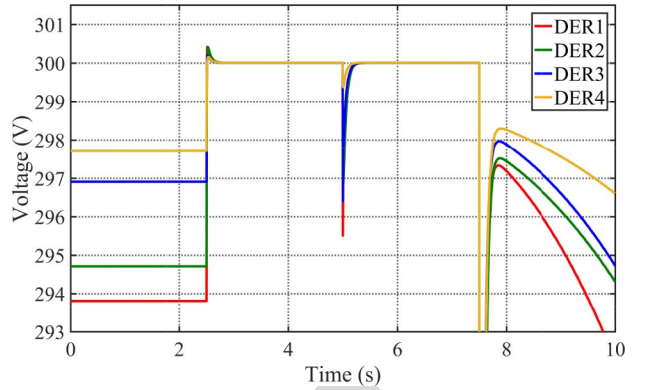


Fig. 8. Voltage tracking performance of feedback linearization control.

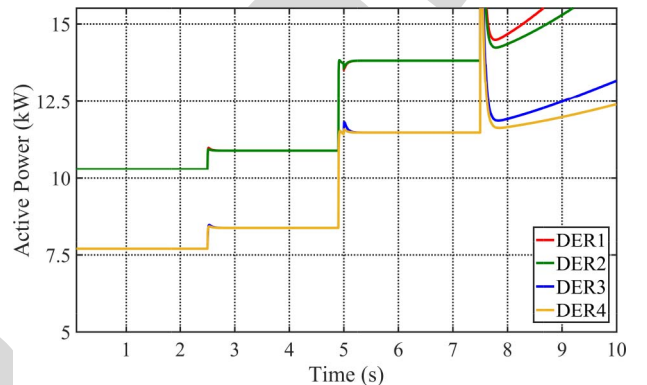


Fig. 9. Active power outputs of DERs with feedback linearization control.

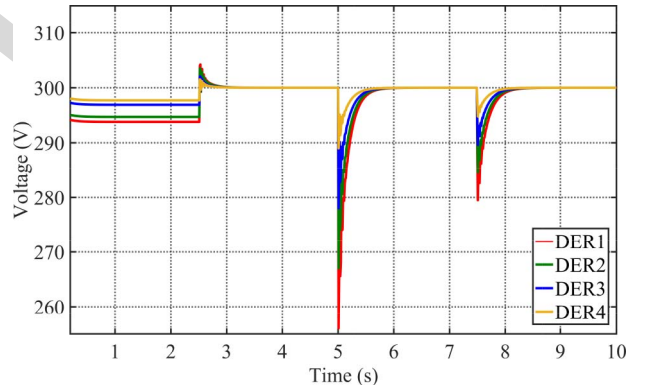


Fig. 10. Voltage tracking performance of PID control.

569 fixing  $j \leftarrow L$ . The results are shown in Fig. 7. Due to the inac-  
 570 curacy of linearized model, the parameters are kept updating  
 571 automatically, which leads to the oscillations of output volt-  
 572 ages. However, the stability is still guaranteed and the errors  
 573 between real and reference voltages are maintained bounded,  
 574 even when large disturbances occur.

#### 575 D. Comparison With Feedback Linearization Control

576 A comparison study with input-output feedback lineariza-  
 577 tion control, which is well-known as nonlinear control method  
 578 requiring precise model, is carried out in this section. When  
 579 load 3 is attached at  $t = 5$  s, we assume the information of  
 580 load change is known by the secondary controller based on  
 581 feedback linearization. Similarly, an unknown parameter per-  
 582 turbation occurs at  $t = 7.5$  s. As shown in Fig. 8, though the  
 583 feedback linearization controller can deal with the *known* large  
 584 load fluctuation, it fails to restore and stabilize the output volt-  
 585 ages in case of *uncertainties*. The corresponding active power  
 586 outputs are shown in Fig. 9.

#### 587 E. Comparison With PID Control

588 To compare the proposed method with the existing model-  
 589 free approaches, in this section, we conduct simulations by  
 590 the most widely-used model-free PID control. Fig. 10 and  
 591 Fig. 11 show that, under the same conditions, the PID control  
 592 can realize accurate voltage tracking and is robust to  
 593 unknown parameter perturbation. However, compared with  
 594 the proposed method, PID control performs more sluggish

595 transient responses and much larger overshootings after large  
 596 load disturbance and parameter perturbation.

#### 597 F. Effect of Time Delays

598 In this section, we test the robustness of the proposed con-  
 599 troller against time delays. The sampling time  $\Delta T = 10$  ms.  
 600 We set the time delays as  $\{(d-1) \times \Delta T | d = 1, 2, 3, 5, 10, 20\}$ ,  
 601 respectively. Any fractional time delays are rounded up. Load  
 602 3 is attached at  $t = 5$  s. Fig. 12 shows the comparison of  
 603 voltage tracking performances with different time delays of  
 604 DER1. The blue line shows the result without time delay,  
 605 i.e.,  $d = 1$ . The red line shows the worst case with a delay  
 606 of 190 ms. The result shows that the proposed controller  
 607 can stabilize the system with any different delays. However,



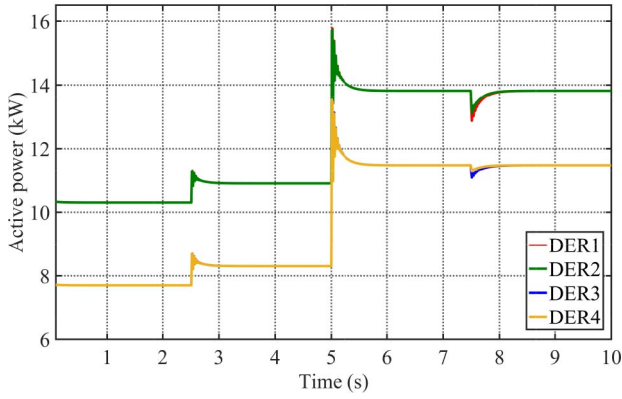


Fig. 11. Active power outputs of DERs with PID control.

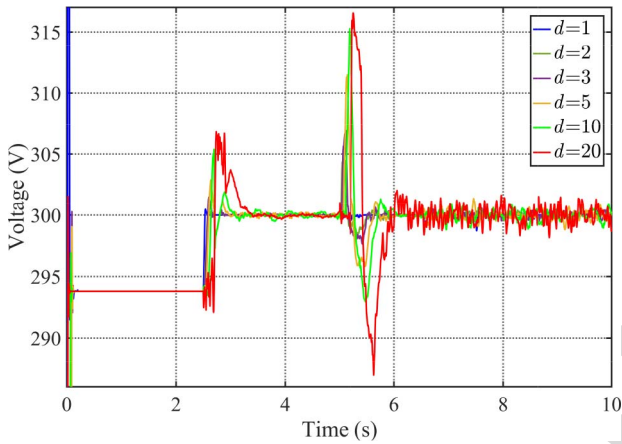


Fig. 12. Voltage tracking performance with different time delays; SVC is applied after 2.5 s; load 3 is attached at 5 s.

608 as time delay increases, the settling time and overshoot of  
609 transient responses become larger. For steady-state operation,  
610 there are larger oscillations under larger time delays.

### 611 G. Effect of Communication Noise Disturbances

612 The noise disturbances in communication links between sec-  
613 ondary and primary levels widely exist in the SVC of MGs  
614 and may degrade the dynamic performance of the controller.  
615 To study the influence of communication noise disturbances on  
616 the proposed SVC method, white noises with signal-to-noise  
617 ratio (SNR) of 30 dB, 20 dB and 10 dB are added to the com-  
618 munication links between SVC and primary level. Note that  
619 smaller SNR indicates larger noise disturbance, and the SNR  
620 is usually between 30 to 40 dB in MGs [50], [51]. As shown in  
621 Fig. 13, the proposed SVC method can realize voltage tracking  
622 and BIBO stability with some ripples under small communi-  
623 cation noise disturbances; however, the dynamic performance  
624 degrades when noise enlarges.

## 625 V. CONCLUSION

626 In this article, we proposed a novel model-free SVC using  
627 nonlinear multiple models adaptive control. The MGs with pri-  
628 mary control are treated as a “black-box” when designing the  
629 SVC. The proposed controller consists of two separate parts,  
630 i.e., LAC and NAC, which are coordinated by a switching  
631 mechanism. The unmodeled nonlinear dynamics are online

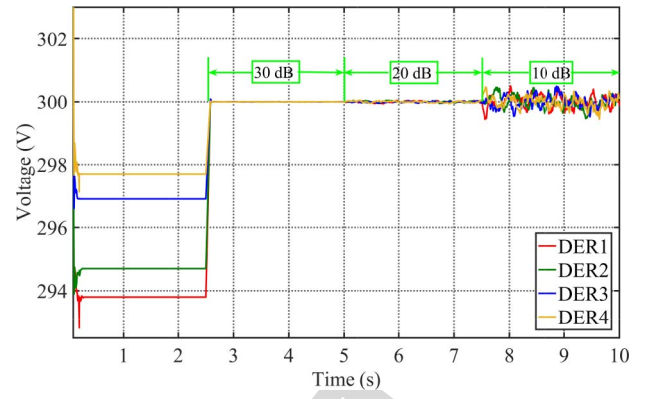


Fig. 13. Voltage tracking performance with different communication noise disturbances. Communication noises with 30 dB, 20 dB and 10 dB SNR are added at 2.5 s, 5 s, and 7.5 s, respectively.

632 estimated by ANNs. We have proved that the tracking errors can  
633 be achieved arbitrarily small given a proper nonlinear identifica-  
634 tion. The simulation results show that such switching mechanism  
635 can guarantee BIBO stability of the closed-loop system while  
636 achieving accurate tracking. The proposed controller is robust  
637 to uncertainties, disturbances and time delays.

638 Due to the advantages of flexibility and robustness, the  
639 distributed and decentralized model-free secondary voltage  
640 control will be further investigated in our future works.

## 641 APPENDIX

642 *Proof of Proposition 1:* This proof can be separated into two  
643 parts: the BIBO stability of output voltage and the convergence  
644 of voltage tracking error. For the proof of stability, we first  
645 prove that SVC input  $\mathbf{E}^*$  and output voltage  $\mathbf{v}_o$  are bounded  
646 by  $\mathbf{e}$ , then we use the contradiction argument to prove that  $\mathbf{e}$   
647 is bounded, and that means  $\mathbf{E}^*$  and  $\mathbf{v}_o$  are also bounded.

648 Define the parameter identification error of linear estimator  
649 as  $\boldsymbol{\psi}_L(k) = \hat{\boldsymbol{\theta}}_L(k) - \boldsymbol{\theta}$ . By (12), it follows that  
649

$$650 \boldsymbol{\psi}_L(k) = \boldsymbol{\psi}_L(k-d) + \frac{\eta_L(k)\boldsymbol{\Psi}(k-d)\mathbf{e}_L(k)^T}{1 + \|\boldsymbol{\Psi}(k-d)\|^2}. \quad (25)$$

651 Following the proof in [41] and from the logic function (22),  
652 it can be proven that  $\hat{\boldsymbol{\theta}}_L(k)$  is bounded. In addition,

$$653 \lim_{N \rightarrow \infty} \sum_{k=d}^N \frac{\eta_L(k)(\|\mathbf{e}_L(k)\|^2 - 4\rho^2)}{2(1 + \|\boldsymbol{\Psi}(k-d)\|^2)} < \infty, \quad (26)$$

$$654 \lim_{k \rightarrow \infty} \frac{\eta_L(k)(\|\mathbf{e}_L(k)\|^2 - 4\rho^2)}{2(1 + \|\boldsymbol{\Psi}(k-d)\|^2)} \rightarrow 0. \quad (27)$$

655 From (14) and (19), we have

$$656 \mathbf{e}_L(k) = \mathbf{F}(z^{-1})\mathbf{v}_o(k) - \mathbf{R}\mathbf{v}_o^{\text{ref}}(k-d). \quad (28)$$

657 Since  $\mathbf{F}(z^{-1})$  is stable, then from (28), there exist positive  
658 constants  $\ell_1$  and  $\ell_2$  such that

$$659 \|\boldsymbol{\Psi}(k-d)\| \leq \ell_1 + \ell_2 \max_{0 \leq \tau \leq k} \|\mathbf{e}_L(\tau)\|. \quad (29)$$

660 which indicates that the input  $\mathbf{E}^*$  and output voltage  $\mathbf{v}_o$  are  
661 bounded by the linear identification error  $\mathbf{e}_L$ .

662 To prove the boundedness of  $\mathbf{e}_L$ , we utilize the proof by  
663 contradiction argument. Suppose that  $\mathbf{e}_L(k)$  is unbounded, then

there must exist a positive time constant  $T$ , such that  $\|e_L(k)\| > 2\rho$  and  $a_L(k) = 1$  for  $k > T$ , i.e., there exists a monotonic increasing sequence  $\|e_L(k_n)\|$  such that  $\lim_{k_n \rightarrow \infty} \|e_L(k_n)\| = \infty$ . Then, it follows that

$$\begin{aligned} & \lim_{k_n \rightarrow \infty} \frac{\eta_L(k_n)(\|e_L(k_n)\|^2 - 4\rho^2)}{2(1 + \|\Psi(k_n - d)\|^2)} \\ & \geq \lim_{k_n \rightarrow \infty} \frac{\eta_L(k_n)(\|e_L(k_n)\|^2 - 4\rho^2)}{2\left(1 + (\ell_1 + \ell_2 \max_{0 \leq \tau \leq k} \|e_L(\tau)\|)^2\right)} \\ & \geq \lim_{k_n \rightarrow \infty} \frac{\eta_L(k_n)(\|e_L(k_n)\|^2 - 4\rho^2)}{2(1 + (\ell_1 + \ell_2 \|e_L(k_n)\|)^2)} \\ & \geq \frac{1}{2\ell_2^2} \\ & > 0. \end{aligned} \quad (30)$$

However, it contradicts (27) which means  $e_L(k)$  is bounded. Thus, it proves the BIBO stability for LAC. For NAC, from (17) and (20), it follows that,

$$e_N(k) = F(z^{-1})v_o(k) - Rv_o^{\text{ref}}(k - d). \quad (31)$$

Since  $F(z^{-1})$  is stable, then from (31), there exist positive constants  $\ell_3$  and  $\ell_4$  such that

$$\|\Psi(k - d)\| \leq \ell_3 + \ell_4 \max_{0 \leq \tau \leq k} \|e_N(\tau)\|. \quad (32)$$

The first term in (21) is bounded according to (26), and the second term is also bounded due to the dead-zone function (22). Hence  $\xi_L(k)$  is bounded. If  $\xi_N(k)$  is bounded, according to the switching mechanism function (21), we have

$$\lim_{k \rightarrow \infty} \frac{\eta_N(k)(\|e_N(k)\|^2 - 4\rho^2)}{2(1 + \|\Psi(k - d)\|^2)} \rightarrow 0. \quad (33)$$

In this case, both of linear or nonlinear identification errors of the closed-loop MG system  $e_j(k)$ ,  $j = \{L, N\}$  satisfy that

$$\lim_{k \rightarrow \infty} \frac{\eta(k)(\|e(k)\|^2 - 4\rho^2)}{2(1 + \|\Psi(k - d)\|^2)} \rightarrow 0, \quad (34)$$

where

$$a(k) = \begin{cases} 1, & \text{if } \|e(k)\| > 2\rho, \\ 0, & \text{otherwise.} \end{cases} \quad (35)$$

If  $\xi_N(k)$  is unbounded, considering  $\xi_L(k)$  is bounded, there must exist  $k_0 > 0$  such that  $\xi_L(k) \leq \xi_N(k)$ ,  $\forall k \geq k_0$ . Then after time  $k_0$ , the switching mechanism will choose the linear controller, thus the identification error  $e(k) = e_L(k)$  which also satisfies (34).

Finally, from (29), (32) and (34), it can be proved that  $v_o$  and  $E^*$  are bounded, i.e., the input and output of the closed-loop switching system are bounded while the identification error  $e_j(k)$  satisfies

$$\lim_{k \rightarrow \infty} \|e_j(k)\| \leq 2\rho, \quad j = \{L, N\} \quad (36)$$

which indicates that there exist positive constants  $\ell_5$  and  $\ell_6$  such that,

$$\|\Psi(k - d)\| \leq \ell_5 + \ell_6 \max_{0 \leq \tau \leq k} \|e_j(\tau)\| \leq \ell_5 + 2\ell_6\rho. \quad (37)$$

Let  $\Delta = \ell_5 + 2\ell_6\rho$ , it follows that

$$\max_{0 \leq \tau \leq k} \{\|v_o(\tau)\|, \|E^*(\tau)\|\} \leq \Delta. \quad (38)$$

Now we have proven the BIBO voltage stability of the closed-loop MG system with the proposed SVC.

*Proof of Proposition 2:* Switching mechanism always selects the controller, with respect to the smaller identification error, as the SVC input for MG system. Moreover, from (28) and (31), the output voltage tracking error  $\bar{e}(k)$  is equivalent to the smaller identification error. From (17), we have the nonlinear identification error,

$$\begin{aligned} e_N(k) &= y_N(k) - \hat{\theta}_N(k - d)^T \Psi(k - d) - \delta \hat{h}[\bar{\Psi}(k - d)] \\ &= y_N(k) - (y_N(k) - \delta h[\bar{\Psi}(k - d)]) - \delta \hat{h}[\bar{\Psi}(k - d)] \\ &= \delta h[\bar{\Psi}(k - d)] - \delta \hat{h}[\bar{\Psi}(k - d)]. \end{aligned} \quad (39)$$

When the hyper-parameters of the ANN are well-tuned, for arbitrary small positive constant  $\epsilon$ , the voltage tracking error always satisfies  $\|\delta h[\bar{\Psi}(k - d)] - \delta \hat{h}[\bar{\Psi}(k - d)]\| < \epsilon$ . It means the nonlinear identification error is always smaller than the linear one, so that the tracking error will be automatically selected as the nonlinear identification error, i.e.,

$$\lim_{k \rightarrow \infty} \|\bar{e}(k)\| = \lim_{k \rightarrow \infty} \|e_N(k)\| < \epsilon. \quad (40)$$

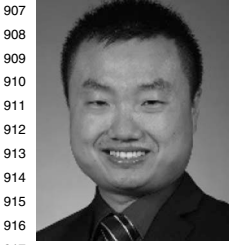
## REFERENCES

- [1] J. C. Vasquez, J. M. Guerrero, J. Miret, M. Castilla, and L. G. de Vicuña, "Hierarchical control of intelligent microgrids," *IEEE Ind. Electron. Mag.*, vol. 4, no. 4, pp. 23–29, Dec. 2010.
- [2] J. M. Guerrero, J. C. Vasquez, J. Matas, L. G. De Vicuña, and M. Castilla, "Hierarchical control of droop-controlled AC and DC microgrids—A general approach toward standardization," *IEEE Trans. Ind. Electron.*, vol. 58, no. 1, pp. 158–172, Jan. 2011.
- [3] A. Bidram and A. Davoudi, "Hierarchical structure of microgrids control system," *IEEE Trans. Smart Grid*, vol. 3, no. 4, pp. 1963–1976, Dec. 2012.
- [4] N. Jumpasri, K. Pinsuntia, K. Woranetsuttikul, T. Nilsakorn, and W. Khan-ngern, "Comparison of distributed and centralized control for partial shading in PV parallel based on particle swarm optimization algorithm," in *Proc. Int. Elect. Eng. Congr. (iEECON)*, Chonburi, Thailand, 2014, pp. 1–4.
- [5] T. Morstyn, B. Hredzak, and V. G. Agelidis, "Distributed cooperative control of microgrid storage," *IEEE Trans. Power Syst.*, vol. 30, no. 5, pp. 2780–2789, Sep. 2015.
- [6] T. Dragicevic, X. Lu, J. C. Vasquez, and J. M. Guerrero, "DC microgrids—Part I: A review of control strategies and stabilization techniques," *IEEE Trans. Power Electron.*, vol. 31, no. 7, pp. 4876–4891, Jul. 2016.
- [7] Q. Shafiee, J. M. Guerrero, and J. C. Vasquez, "Distributed secondary control for islanded microgrids—A novel approach," *IEEE Trans. Power Electron.*, vol. 29, no. 2, pp. 1018–1031, Feb. 2014.
- [8] J. W. Simpson-Porco, F. Dörfler, and F. Bullo, "Synchronization and power sharing for droop-controlled inverters in islanded microgrids," *Automatica*, vol. 49, no. 9, pp. 2603–2611, Dec. 2013.
- [9] B. Wei, Y. Gui, S. Trujillo, J. M. Guerrero, J. C. Vásquez, and A. Marzábal, "Distributed average integral secondary control for modular ups systems-based microgrids," *IEEE Trans. Power Electron.*, vol. 34, no. 7, pp. 6922–6936, Jul. 2019.
- [10] Q. Shafiee, Č. Stefanović, T. Dragičević, P. Popovski, J. C. Vasquez, and J. M. Guerrero, "Robust networked control scheme for distributed secondary control of islanded microgrids," *IEEE Trans. Ind. Electron.*, vol. 61, no. 10, pp. 5363–5374, Oct. 2014.
- [11] A. Bidram, A. Davoudi, F. L. Lewis, and Z. Qu, "Secondary control of microgrids based on distributed cooperative control of multi-agent systems," *IET Gener. Transm. Distrib.*, vol. 7, no. 8, pp. 822–831, Aug. 2013.

- [12] A. Bidram, A. Davoudi, F. L. Lewis, and S. S. Ge, "Distributed adaptive voltage control of inverter-based microgrids," *IEEE Trans. Energy Convers.*, vol. 29, no. 4, pp. 862–872, Dec. 2014.
- [13] Y. Guo, H. Gao, and Q. Wu, "Distributed cooperative voltage control of wind farms based on consensus protocol," *Int. J. Elect. Power Energy Syst.*, vol. 104, pp. 593–602, Jan. 2019.
- [14] Z. Ma, Z. Wang, and Y. Yuan, Y. Wang, R. Diao, and D. Shi, "Stability and accuracy assessment based large-signal order reduction of microgrids," 2019. [Online]. Available: arXiv:1910.03687.
- [15] A. Bidram, A. Davoudi, F. L. Lewis, and J. M. Guerrero, "Distributed cooperative secondary control of microgrids using feedback linearization," *IEEE Trans. Power Syst.*, vol. 28, no. 3, pp. 3462–3470, Aug. 2013.
- [16] C. Ahumada, R. Cárdenas, D. Sáez, and J. M. Guerrero, "Secondary control strategies for frequency restoration in islanded microgrids with consideration of communication delays," *IEEE Trans. Smart Grid*, vol. 7, no. 3, pp. 1430–1441, May 2016.
- [17] M. Mokhtar, M. I. Marei, and A. A. El-Sattar, "An adaptive droop control scheme for DC microgrids integrating sliding mode voltage and current controlled boost converters," *IEEE Trans. Smart Grid*, vol. 10, no. 2, pp. 1685–1693, Mar. 2019.
- [18] C. Wang, P. Yang, C. Ye, Y. Wang, and Z. Xu, "Voltage control strategy for three/single phase hybrid multimicrogrid," *IEEE Trans. Energy Convers.*, vol. 31, no. 4, pp. 1498–1509, Dec. 2016.
- [19] M. J. Hossain, M. A. Mahmud, F. Milano, S. Bacha, and A. Hably, "Design of robust distributed control for interconnected microgrids," *IEEE Trans. Smart Grid*, vol. 7, no. 6, pp. 2724–2735, Nov. 2016.
- [20] F. Guo, C. Wen, J. Mao, and Y. Song, "Distributed secondary voltage and frequency restoration control of droop-controlled inverter-based microgrids," *IEEE Trans. Ind. Electron.*, vol. 62, no. 7, pp. 4355–4364, Jul. 2015.
- [21] H. Cai, G. Hu, F. L. Lewis, and A. Davoudi, "A distributed feedforward approach to cooperative control of AC microgrids," *IEEE Trans. Power Syst.*, vol. 31, no. 5, pp. 4057–4067, Sep. 2016.
- [22] N. M. Dehkordi, N. Sadati, and M. Hamzeh, "Distributed robust finite-time secondary voltage and frequency control of islanded microgrids," *IEEE Trans. Power Syst.*, vol. 32, no. 5, pp. 3648–3659, Sep. 2017.
- [23] A. H. Etemadi, E. J. Davison, and R. Iravani, "A decentralized robust control strategy for multi-DER microgrids—Part I: Fundamental concepts," *IEEE Trans. Power Del.*, vol. 27, no. 4, pp. 1843–1853, Oct. 2012.
- [24] T. Geyer and D. E. Quevedo, "Multistep finite control set model predictive control for power electronics," *IEEE Trans. Power Electron.*, vol. 29, no. 12, pp. 6836–6846, Dec. 2014.
- [25] M. Davari and Y. A. I. Mohamed, "Variable-structure-based nonlinear control for the master VSC in DC-energy-pool multiterminal grids," *IEEE Trans. Power Electron.*, vol. 29, no. 11, pp. 6196–6213, Nov. 2014.
- [26] J. Lai, X. Lu, and X. Yu, "Stochastic distributed frequency and load sharing control for microgrids with communication delays," *IEEE Syst. J.*, vol. 13, no. 4, pp. 4269–4280, Dec. 2019.
- [27] J. Lai, X. Lu, X. Yu, and A. Monti, "Stochastic distributed secondary control for AC microgrids via event-triggered communication," *IEEE Trans. Smart Grid*, vol. 11, no. 4, pp. 2746–2759, Jul. 2020.
- [28] M. Khooban, "Secondary load frequency control of time-delay stand-alone microgrids with electric vehicles," *IEEE Trans. Ind. Electron.*, vol. 65, no. 9, pp. 7416–7422, Sep. 2018.
- [29] H. Zhang, J. Zhou, Q. Sun, J. M. Guerrero, and D. Ma, "Data-driven control for interlinked AC/DC microgrids via model-free adaptive control and dual-droop control," *IEEE Trans. Smart Grid*, vol. 8, no. 2, pp. 557–571, Mar. 2017.
- [30] C. Ahn and H. Peng, "Decentralized voltage control to minimize distribution power loss of microgrids," *IEEE Trans. Smart Grid*, vol. 4, no. 3, pp. 1297–1304, Sep. 2013.
- [31] M. Khooban *et al.*, "Robust frequency regulation in mobile microgrids: HIL implementation," *IEEE Syst. J.*, vol. 13, no. 4, pp. 4281–4291, Dec. 2019.
- [32] V. Utkin, "Discussion aspects of high-order sliding mode control," *IEEE Trans. Autom. Control*, vol. 61, no. 3, pp. 829–833, Mar. 2016.
- [33] J. W. Simpson-Porco, Q. Shafiq, F. Dörfler, J. C. Vasquez, J. M. Guerrero, and F. Bullo, "Secondary frequency and voltage control of islanded microgrids via distributed averaging," *IEEE Trans. Ind. Electron.*, vol. 62, no. 11, pp. 7025–7038, Nov. 2015.
- [34] H. Zhang, C. Qin, B. Jiang, and Y. Luo, "Online adaptive policy learning algorithm for  $h_\infty$  state feedback control of unknown affine nonlinear discrete-time systems," *IEEE Trans. Cybern.*, vol. 44, no. 12, pp. 2706–2718, Dec. 2014.
- [35] H. Zhang and Y. Quan, "Modeling, identification, and control of a class of nonlinear systems," *IEEE Trans. Fuzzy Syst.*, vol. 9, no. 2, pp. 349–354, Apr. 2001.
- [36] T. Sreekumar and K. S. Jiji, "Comparison of proportional-integral (P-I) and integral-proportional (I-P) controllers for speed control in vector controlled induction motor drive," in *Proc. 2nd Int. Conf. Power Control Embedded Syst.*, Allahabad, India, Dec. 2012, pp. 1–6.
- [37] N. Kroutikova, C. A. Hernandez-Aramburo, and T. C. Green, "State-space model of grid-connected inverters under current control mode," *IET Elect. Power Appl.*, vol. 1, no. 3, pp. 329–338, May 2007.
- [38] Y. Fu and T. Chai, "Nonlinear multivariable adaptive control using multiple models and neural networks," *Automatica*, vol. 43, no. 6, pp. 1101–1110, Jun. 2007.
- [39] D. Erdogmus, J. Cho, J. Lan, M. Motter, and J. C. Principe, "Adaptive local linear modelling and control of nonlinear dynamical systems," *IEE Control Eng. Series*, vol. 70, p. 119, Jul. 2005.
- [40] Y. Zhang, T. Chai, H. Wang, J. Fu, L. Zhang, and Y. Wang, "An adaptive generalized predictive control method for nonlinear systems based on anfis and multiple models," *IEEE Trans. Fuzzy Syst.*, vol. 18, no. 6, pp. 1070–1082, Dec. 2010.
- [41] L. Chen and K. S. Narendra, "Nonlinear adaptive control using neural networks and multiple models," *Automatica*, vol. 37, no. 8, pp. 1245–1255, Aug. 2001.
- [42] K.-I. Funahashi, "On the approximate realization of continuous mappings by neural networks," *Neural Netw.*, vol. 2, no. 3, pp. 183–192, 1989.
- [43] H. Larochelle, D. Erhan, A. Courville, J. Bergstra, and Y. Bengio, "An empirical evaluation of deep architectures on problems with many factors of variation," in *Proc. 24th Int. Conf. Mach. Learn.*, 2007, pp. 473–480.
- [44] J. Li, Z. Ma, and J. Fu, "Exponential stabilization of switched discrete-time systems with all unstable modes," *Asian J. Control*, vol. 20, no. 1, pp. 608–612, Sep. 2018.
- [45] J. Lai, X. Lu, X. Yu, A. Monti, and H. Zhou, "Distributed voltage regulation for cyber-physical microgrids with coupling delays and slow switching topologies," *IEEE Trans. Syst., Man, Cybern., Syst.*, vol. 50, no. 1, pp. 100–110, Jan. 2020.
- [46] C. Zhao, W. Sun, J. Wang, Q. Li, D. Mu, and X. Xu, "Distributed cooperative secondary control for islanded microgrid with Markov time-varying delays," *IEEE Trans. Energy Convers.*, vol. 34, no. 4, pp. 2235–2247, Dec. 2019.
- [47] A. C. Z. de Souza and M. Castilla, *Microgrids Design and Implementation*. Cham, Switzerland: Springer, 2019.
- [48] A. Bidram, F. L. Lewis, and A. Davoudi, "Distributed control systems for small-scale power networks: Using multiagent cooperative control theory," *IEEE Control Syst. Mag.*, vol. 34, no. 6, pp. 56–77, Dec. 2014.
- [49] M. T. Hagan and M. B. Menhaj, "Training feedforward networks with the Marquardt algorithm," *IEEE Trans. Neural Netw.*, vol. 5, no. 6, pp. 989–993, Nov. 1994.
- [50] E. Casagrande, W. L. Woon, H. H. Zeineldin, and D. Svetinovic, "A differential sequence component protection scheme for microgrids with inverter-based distributed generators," *IEEE Trans. Smart Grid*, vol. 5, no. 1, pp. 29–37, Jan. 2014.
- [51] J. J. Q. Yu, Y. Hou, A. Y. S. Lam, and V. O. K. Li, "Intelligent fault detection scheme for microgrids with wavelet-based deep neural networks," *IEEE Trans. Smart Grid*, vol. 10, no. 2, pp. 1694–1703, Mar. 2019.



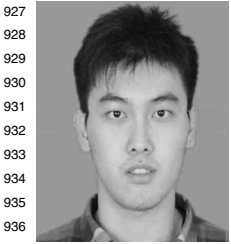
**Zixiao Ma** (Graduate Student Member, IEEE) received the B.S. degree in automation and the M.S. degree in control theory and control engineering from Northeastern University in 2014 and 2017, respectively. He is currently pursuing the Ph.D. degree with the Department of Electrical and Computer Engineering, Iowa State University, Ames, IA, USA. His research interests are focused on the power system load modeling, microgrids, nonlinear control, and model reduction.



907 **Zhaoyu Wang** (Member, IEEE) received the B.S. and M.S. degrees in electrical engineering from Shanghai Jiao Tong University in 2009 and 2012, respectively, and the M.S. and Ph.D. degrees in electrical and computer engineering from the Georgia Institute of Technology in 2012 and 2015, respectively. He is the Harpole-Pentair Assistant Professor with Iowa State University. His research interests include power distribution systems and microgrids, particularly on their data analytics and optimization. He is the Principal Investigator for a multitude of projects focused on these topics and funded by the National Science Foundation, the Department of Energy, National Laboratories, PSERC, and Iowa Energy Center. He is the Secretary of IEEE Power and Energy Society (PES) Award Subcommittee, the Co-Vice Chair of PES Distribution System Operation and Planning Subcommittee, and the Vice Chair of PES Task Force on Advances in Natural Disaster Mitigation Methods. He is an Editor of the IEEE TRANSACTIONS ON POWER SYSTEMS, the IEEE TRANSACTIONS ON SMART GRID, IEEE PES Letters, and the IEEE OPEN ACCESS JOURNAL OF POWER AND ENERGY, and an Associate Editor of *IET Smart Grid*.



940 **Yuxuan Yuan** (Member, IEEE) received the B.S. degree in electrical and computer engineering from Iowa State University, Ames, IA, in 2017, where he is currently pursuing the Ph.D. degree. His research interests include distribution system state estimation, synthetic networks, data analytics, and machine learning.



927 **Yifei Guo** (Member, IEEE) received the B.E. and Ph.D. degrees in electrical engineering from Shandong University, Jinan, China, in 2014 and 2019, respectively. He is currently a Postdoctoral Research Associate with the Department of Electrical and Computer Engineering, Iowa State University, Ames, IA, USA. He was a visiting student with the Department of Electrical Engineering, Technical University of Denmark, Lyngby, Denmark, from 2017 to 2018. His research interests include voltage/var control, renewable energy integration, distribution system optimization and control, and power system protection.



947 **Hao Chen** (Member, IEEE) received the B.S. degree in electrical engineering from the Nanjing University of Science and Technology, Nanjing, China, in 2008, the M.S. degree in electrical engineering from the Illinois Institute of Technology, Chicago, in 2010, and the Ph.D. degree in electrical engineering from the Georgia Institute of Technology in 2016. From 2010 to 2012, he was an Electrical Engineer with Varentec, San Jose, CA, where he worked on various projects, including solid state transformers, dynamic VAR compensators, and voltage compensation for distribution system. He is currently a Staff Electronic Design Engineer with Tesla.

## AUTHOR QUERIES

### AUTHOR PLEASE ANSWER ALL QUERIES

**PLEASE NOTE:** We cannot accept new source files as corrections for your paper. If possible, please annotate the PDF proof we have sent you with your corrections and upload it via the Author Gateway. Alternatively, you may send us your corrections in list format. You may also upload revised graphics via the Author Gateway.

Carefully check the page proofs (and coordinate with all authors); additional changes or updates **WILL NOT** be accepted after the article is published online/print in its final form. Please check author names and affiliations, funding, as well as the overall article for any errors prior to sending in your author proof corrections. Your article has been peer reviewed, accepted as final, and sent in to IEEE. No text changes have been made to the main part of the article as dictated by the editorial level of service for your publication.

AQ1: According to our records, Zixiao Ma is listed as a Graduate Student Member, IEEE.

However, the files provided list them as a Student Member, IEEE. Please verify.

AQ2: According to our records, Yuxuan Yuan is listed as a Member, IEEE. However, the files provided list them as a Student Member, IEEE. Please verify.

AQ3: Please confirm or add details for any funding or financial support for the research of this article.

AQ4: Please provide the department name for Tesla.

AQ5: Please confirm if the location and publisher information for Reference [47] is correct as set.